




Article

A Molecular Dynamics Study of the Generation of Ethanol for Insulating Paper Pyrolysis [†]

Yiyi Zhang ^{*}, Yi Li, Shizuo Li ^{*}, Hanbo Zheng  and Jiefeng Liu 

Department of Electrical Engineering, Guangxi University, Nanning 530004, China; yili665143@163.com (Y.L.); hanbozheng@163.com (H.Z.); liujiefeng9999@163.com (J.L.)

^{*} Correspondence: yiyizhang@gxu.edu.cn (Y.Z.); lsz134679@126.com (S.L.)

[†] This paper is an extended version of our paper published in 2019 ADVANCED RESEARCH WORKSHOP ON TRANSFORMERS Conference, Cordoba, Spain, 7–9 October 2019.

Received: 10 December 2019; Accepted: 4 January 2020; Published: 5 January 2020



Abstract: Cellulosic insulation paper is usually used in oil-immersed transformer insulation systems. In this study, the molecular dynamics method based on reaction force field (ReaxFF) was used to simulate the pyrolysis process of a cellobiose molecular model. Through a series of ReaxFF- Molecular Dynamics (MD) simulations, the generation path of ethanol at the atomic level was studied. Because the molecular system has hydrogen bonding, force-bias Monte Carlo (fbMC) is mixed into ReaxFF to reduce the cost of calculation by reducing the sampled data. In order to ensure the reliability of the simulation, a model composed of 20 cellobioses and a model composed of 40 cellobioses were respectively established for repeated simulation in the range of 500–3000 K. The results show that insulating paper produced ethanol at extreme thermal fault, and the intermediate product of vinyl alcohol is the key to the aging process. It is also basically consistent with others' previous experiment results. So it can provide an effective reference for the use of ethanol as an indicator to evaluate the aging condition of transformers.

Keywords: ethanol; insulating paper; ReaxFF; cellobiose; pyrolysis; molecular dynamics

1. Introduction

With the increasing of the environmental and economical awareness in the energy transmission system, the reliability and economical operation of the power transmission equipment become more and more important in the future [1,2]. Mineral-oil-immersed transformers are widely used in high-voltage transmission systems due to their high insulation strength and long service life. The safe and reliable operation of power systems depends on the condition monitoring and timely maintenance of power transmission and transformation equipment [3]. As the key equipment of power transmission and distribution, the failure of the transformer may lead to serious power system accidents [4,5]. In the event of an extreme transformer failure, its internal temperature can reach more than 700 °C [5]. It results in the irreversible aging of the oil-paper insulation system and then induces various faults. Paper/oil insulation systems include insulating oil and insulating paper. Insulation oil can be purified periodically by regeneration, reconditioning, or changing. However, insulating paper cannot be replaced, it is of great significance to detect the aging status of insulating paper [6]. The degree of polymerization (DP) is the direct parameter to evaluate the aging status of insulating paper. However, the DP cannot be directly measured in the actual transformer operation [7,8]. The aging of insulating paper will produce a variety of products, such as CO, CO₂, acids, low molecular acids, water, aldehydes, and alcohols. Furfural indicator is one of the common methods to evaluate the transformer aging condition. It is susceptible to various operating conditions and cannot accurately reflect the aging situation of local hot spots [9]. Thus, it is of great significance to seek some aging indicators that

can compensate for the existing aging indicators to improve the accuracy of transformer insulation aging evaluation.

Jalbert et al. isolated and identified more than 30 products of aging degradation of insulating paper by gas chromatography-mass spectrometry (GC-MS) [10]. Their results showed that ethanol was a relatively stable aging degradation product of insulating paper. It also showed that an ethanol indicator could be used to characterize the degradation of insulating paper performance [10]. The research results of Fernandez et al. were also consistent with this view [11]. Matharage et al. used gas chromatography and ion trap mass spectrometer to detect methanol in aging insulating paper [12]. Jalbert et al. also summarized methanol had a role as an indicator of cellulosic solid insulation aging in transformer mineral oil, and it was expected that in the future it would be in routine use by utilities [13]. Rodriguez-Celis et al. found that the presence of ethanol during transformer oil analysis was of high interest because it can be related to a thermal fault or hot spot within the solid insulation [14]. Some studies adopt an experimental analysis method, which cannot reflect the mechanism of producing ethanol.

In recent years, with the development of molecular simulation technology, many chemical micro phenomena can be better described. The calculation method based on quantum mechanics is a method to study chemical reactions with high precision, which is widely used in exploration of the process of biomass conversion reaction [15]. However, the use of the quantum mechanics method has certain limitations because of the huge amount of calculation, the range of application in 100 atoms model, and the shorter dimension [16]. Duin et al. proposed a molecular reactive dynamics field named ReaxFF. In contrast to previous molecular simulations in the literatures, the ReaxFF was used to describe the atomic interactions, which allows dynamic bond scission and bond formation [17]. The ReaxFF-MD method can clearly describe the structural changes of reactants and reveal the reaction mechanism. It has been increasingly applied in many monomolecular systems and complex molecular systems. Paajanen et al. used the ReaxFF-MD method to study high-temperature decomposition of the cellulose molecule [18]. Zheng et al. used ReaxFF molecular dynamics to reveal the initial reaction mechanism of cellulose pyrolysis [19]. Zhang et al. used ReaxFF-MD to study the pyrolysis mechanism of oleic-type triglycerides [20]. In conclusion, the ReaxFF-MD method has extensive application, and it provides a new approach for the research of transformer aging mechanisms in the electrical field.

The degradation of insulating paper performance mainly comes from thermal aging. Because the local hot spot fault has the characteristics of instantaneous high temperature, high temperature pyrolysis is used to accelerate thermal aging, instead of oxidation/hydrolysis. The aging mechanism of insulating paper can be obtained by simulating the pyrolysis of insulating paper at the atomic level. In this paper, the ReaxFF-MD method is used for the calculation of the insulation paper in oil-immersed transformer insulation systems, and studies the formation path and the performance of ethanol in the transformer aging process. So it provides theoretical support for ethanol as the new indicator of transformer aging by analyzing the feasibility of ethanol as a new indicator of transformer aging.

2. Methods

2.1. Model Construction

A suitable molecular model is very important for reaction molecular dynamics. Moreover, it is impractical to build a model that is completely consistent with the reality. An approximate model can not only get the correct calculation results, but also reduce the difficulty of building the model. Cellulose is the main component of the insulation paper. In addition, cellobiose is the repeating unit of cellulose [21], and the DP of new insulation paper is between 1000 and 1200 [22]. However, it is impractical to model molecules with thousands of DPs directly. Mezeau had simulated on the different DP value and then found that DP had no impact on the simulation results [23]. Hence, this paper aimed to study the generation path of ethanol molecules. In order to save calculation cost, a molecular

model with repetitive unit (cellobiose) was established. The major atoms of cellobiose were labeled for analysis, which was shown in Figure 1.

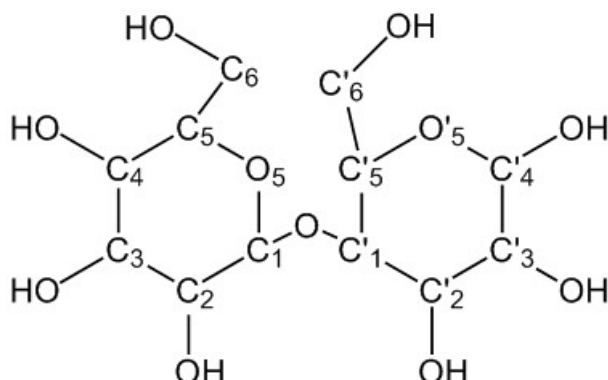


Figure 1. The labeling diagram of cellobiose.

2.2. ReaxFF Principle

The ReaxFF reaction field calculates the bond order of two atoms by the distance. Then it determines the connection of two atoms by the bond order at the current moment. ReaxFF divides the general system energy (E_{system}) into various potential energy contributions [17], as can be expressed as in Equation (1). E_{bond} denotes the bond energy. E_{val} and E_{pen} denote valence angle and penalty energy terms. E_{tors} denotes torsion angle energy. E_{conj} denotes the contribution of conjugation effects to molecular energy. E_{over} and E_{under} denote the atom over-coordination and under-coordination terms. E_{vdWaals} denotes non-bonded van der Waals interactions, and E_{Coulomb} denotes Coulomb interactions. The ReaxFF potential function calculates the distance between atoms and the bond positions at the next moment according to the changes of atomic parameters. Then it determines the connection between the atoms. Finally, it judges the formation or fracture of chemical bonds in molecules. Therefore, the cyclic iteration method is used to simulate the chemical reaction process.

$$E_{\text{system}} = E_{\text{bond}} + E_{\text{over}} + E_{\text{under}} + E_{\text{val}} + E_{\text{pen}} + E_{\text{tors}} + E_{\text{conj}} + E_{\text{vdWaals}} + E_{\text{Coulomb}} \quad (1)$$

2.3. Simulation Details

In this paper, Amsterdam Modeling Suite (AMS) [24], a molecular dynamics simulation software, is used to simulate the pyrolysis of oil-immersed transformer insulating paper [25]. A molecular model of cellobiose was established according to the labeling diagram of cellobiose as shown in Figure 2a. The carbon atom is black, oxygen atom is red, and hydrogen atom is white. Molecular Orbital Package [26] was used for initial optimization of molecules. In order to make the initial optimized molecules more reasonable, the Amsterdam Density Functional (ADF) module is used for geometry optimization. Because cellobiose molecules contain only C, H, and O elements, the generalized gradient approximation-Perdew-Burke-Ernzerhof (GGA-PBE) functional and double zeta + 1 polarization function (DZP) basis set was selected. The optimized cellobiose molecule is shown in Figure 2b and the related energy minimization curve is shown in Figure 3.

A molecular model with a density of 0.69 g/cm^3 was built, which respectively contained 20, 40, and 60 cellobiose molecules as shown in Figure 4a. Geometric optimization was carried out under the isothermal-isobaric ensemble (NPT), and the density of the model was adjusted to 1.59 g/cm^3 after equilibrium stability [27]. Finally, relaxation optimization was carried out on the optimized model under the canonical ensemble (NVT). After the geometry and relaxation optimization of the system, an initial amorphous cell respectively containing 20 and 40 cellobioses was established, the energy was minimized and the density of model was adjusted to 1.59 g/cm^3 [28]. After the above treatment, the established molecular model was consistent with the actual situation, as shown in Figure 4b.

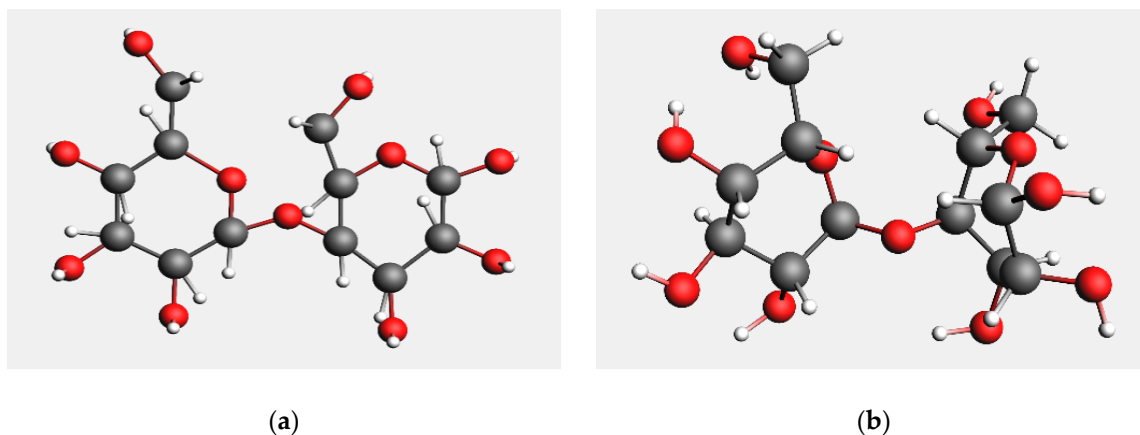


Figure 2. (a) The initial cellobiose; (b) the optimized cellobiose.

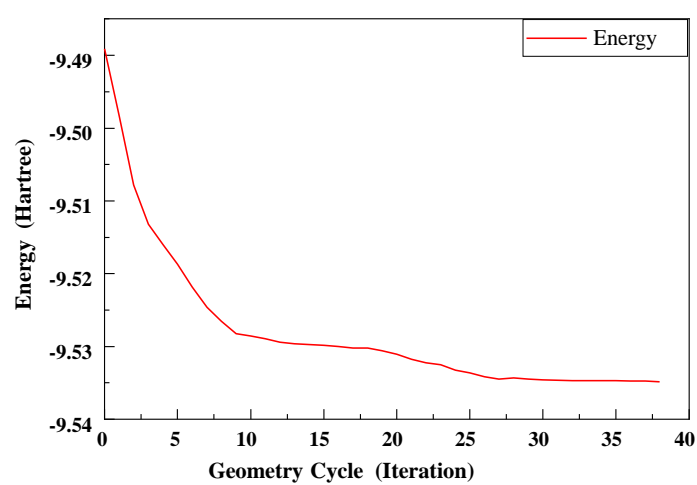


Figure 3. The energy minimization curve of cellobiose.

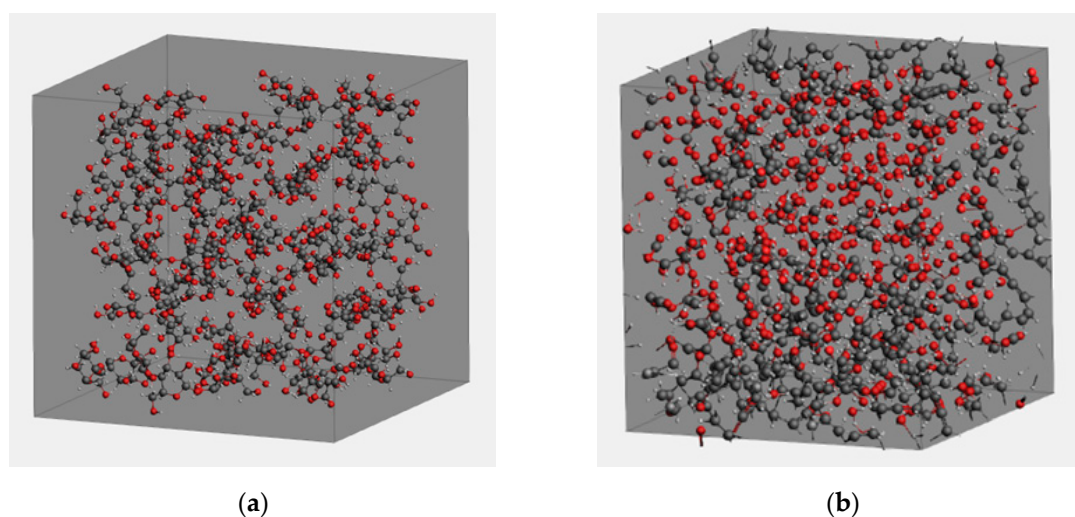


Figure 4. (a) The initial molecular model; (b) the optimized molecular model.

ReaxFF sets up different force fields according to the different elements of the simulation system. A matching force field can make the calculation more accurate. The object of this paper only contained C, H, and O elements, so the CHO field [29] of the ReaxFF module was used in all the simulation processes involved. As the transformer in the aging process, the volume was unchanged. The NVT was used to simulate the pyrolysis at high temperature. Sorensen and Voter proposed a dynamic

method of temperature acceleration based on the transition state theory [30]. Molecular dynamics involves the concepts of bond energy and barrier. In addition, both the bond energy and barrier are independent of temperature, and they are the same as long as they are in the same channel. The essence of temperature is the kinetic energy of the internal vibration of molecules and atoms in molecular dynamics, as well as the kinetic energy of the overall translational motion. The method speeds up the molecular transition by raising the temperature, but only allows events to occur at the same temperature as the original. Therefore, the simulation time scale of this method can be extended on one order of magnitude compared with the conventional molecular dynamics. It can maintain the correct dynamic behavior of the original temperature. On the premise of saving calculation cost and keeping reasonable, this simulation modeled in the temperature range of 500–3000 K. In order to ensure the simulation reliability of each model, the other parameters except temperature should be consistent. The simulation duration was set to 100 ps, time step was set to 0.1 fs, and data was recorded every 10 fs. Because this simulation system contained hydrogen bonds, fbMC mixed into ReaxFF made the calculation of molecular system more effective and accurate. The simulation started fbMC every 500 ReaxFF-MD steps, and fbMC ran 500 steps each time.

2.4. Solubility in Mixture

The COSMO-RS module of AMS was used to calculate the thermodynamic properties of ethanol in insulating oil [31,32]. The mole fraction of insulating oil composition should be 1.0 [33]. The solute (ethanol) should have zero molar fraction in the insulating oil. It was possible to calculate the solubility of a solute at a temperature range. The insulating oils consisted of alkane ($C_{20}H_{42}$), bicyclic alkane ($C_{20}H_{38}$), and dicyclic aromatic hydrocarbon ($C_{20}H_{26}$). Its component models are shown in Figure 5a–c and the ethanol model is shown in Figure 5d. The ratio of alkane, bicyclic alkane, and dicyclic aromatic hydrocarbon was set as 6:3:1 according to the composition of mineral insulating oil. The temperature range of the study was set to 298.15 K to 413.15 K (25–140 °C). The stability of ethanol in oil was studied by the solubility of ethanol at various temperatures.

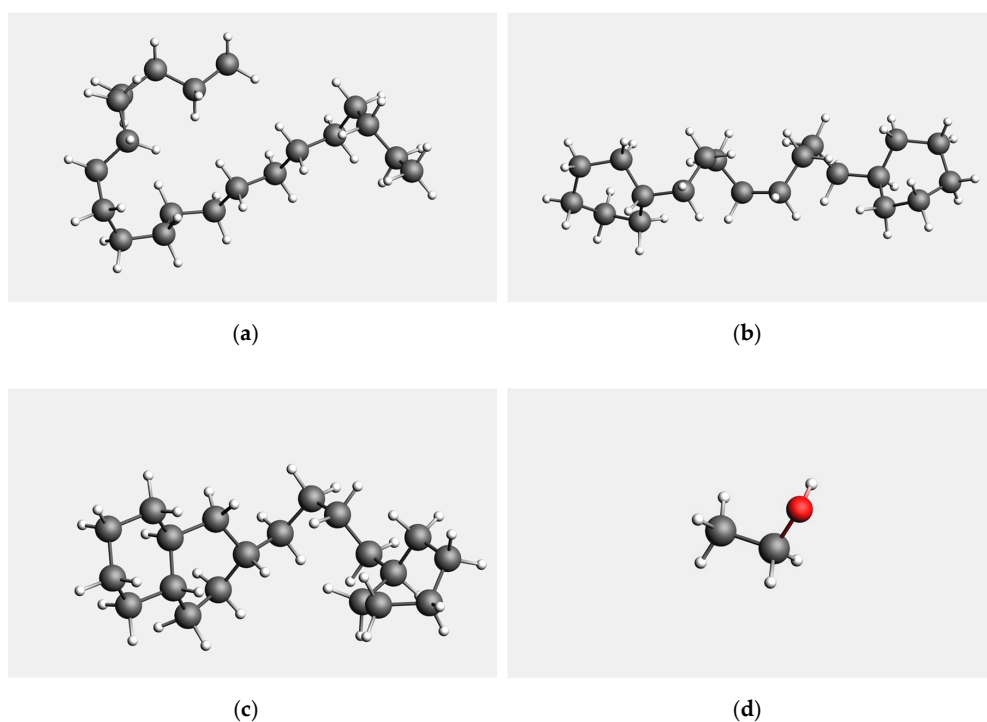


Figure 5. (a) The molecular model of alkanes ($C_{20}H_{42}$); (b) the molecular model of bicyclic alkane ($C_{20}H_{38}$); (c) the molecular model of dicyclic aromatic hydrocarbons ($C_{20}H_{26}$); (d) the molecular model of ethanol.

3. Results and Discussion

3.1. Simulation Results of Cellobiose

In the simulation of the cellobiose molecular model, Figures 6 and 7 show that the curve of different cellobioses to produce ethanol molecules changed with time at different temperatures. For cellobiose samples of 20, no ethanol was produced below 3000 K. For cellobiose samples of 40, no ethanol was found at 2400 K and below, but there were some ethanol molecules at 2600 K, 2800 K, and 3000 K. Analyzing the above graph (Figures 6 and 7) of the pyrolysis, it shows that ethanol was generated stably only at middle and later stages even under the condition of sufficient samples and 2600 K high temperature. The simulation results show that the increase of temperature can accelerate the production of ethanol. Thus, it is speculated that ethanol, as a new indicator, can more accurately characterize the aging state of local winding hot spots in the actual oil-immersed transformer operation, especially in the case of local high-temperature thermal fault. Comparing with 2FAL indicator, it is an advantage for ethanol.

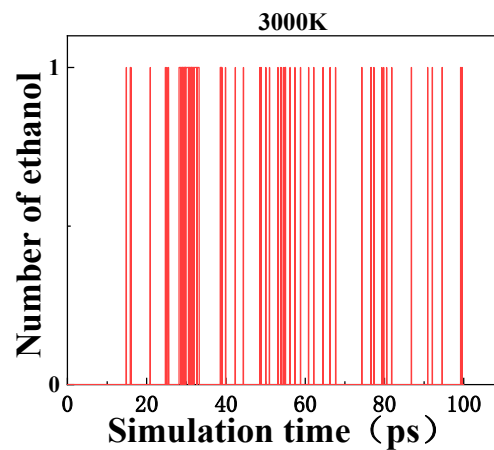


Figure 6. The curve of 20 cellobioses to produce ethanol molecules.

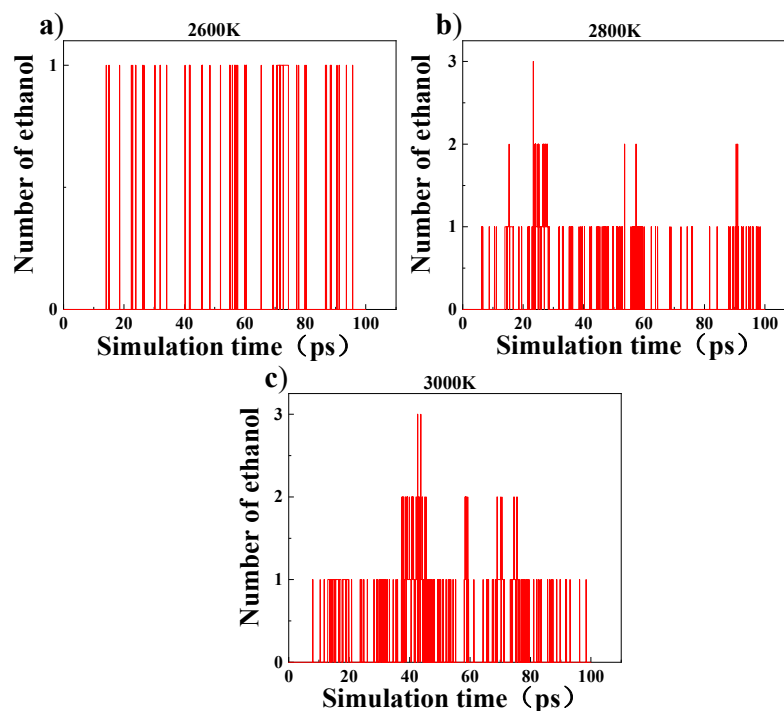


Figure 7. The curve of 40 cellobioses to produce ethanol molecules.

3.2. Analysis on the Formation Path of Ethanol

The fracture and formation of reactant molecular bonds at different simulation moments were observed through the molecular movement trajectory of cellobiose pyrolysis. Then the formation path of an ethanol molecule was analyzed. The relevant path of ethanol production is shown in Figure 8.

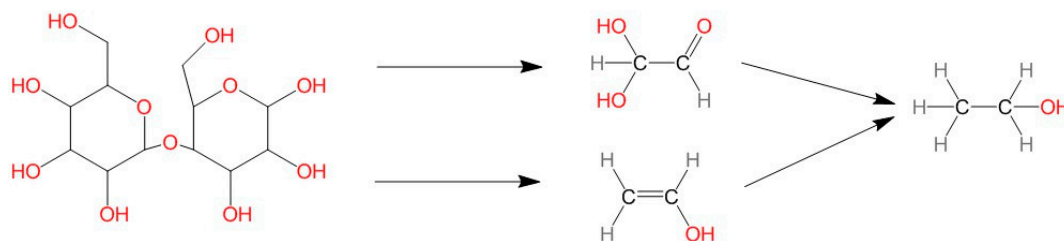


Figure 8. The curve of ethanol molecules.

For the convenience of analysis, the simulated image is enlarged locally. Then, the specific groups of molecules are highlighted or marked with dotted circles. The broken bonds are dotted. The path to generate ethanol is as follows:

In the case of 2800 K, by tracing the source of the formation of ethanol molecules, it can be found that the main part of the formation of ethanol molecules comes from the $-CH_2-$ group connected with C'_5 in the 4-pyran ring of cellobiose. As shown in Figure 9a, at 0.1 ps, glycolaldehyde was generated after the $C'_1-C'_5$ and $C'_4-C'_5$ bond was broken. And then, glyoxal was generated after the H atom connected with C'_6 and the H atom of hydroxyl were captured from glycolaldehyde at 0.9 ps as shown in Figure 9b. Because the chemical character of glyoxal was active and extremely unstable, its two aldehyde groups gained H atoms so that it formed $HOCH=CHOH$, which was unstable. As shown in Figure 9c, acetylene was generated after $HOCH=CHOH$ lost two hydroxyl groups at 3.47 ps. But the chemical character of acetylene was also active, its two carbon atoms captured H atom and $-OH$ respectively, and then vinyl alcohol was generated at 9.2 ps. As shown in Figure 9d, because of the instability of the vinyl alcohol, ethanol was generated after its two C atoms both captured H atoms from nearby carbon oxides at 13.95 ps. At 2600 K and 3000 K, the cellobiose was also converted into vinyl alcohol, but at these two temperatures, vinyl alcohol reacted with free radicals to produce ethylene, as shown in Figure 9e. Ethylene continued to capture the hydroxyl group from the carbon oxide, as shown in Figure 9f. Because of its unstable structure, the H atom from the nearby chain hydrocarbons was finally captured to form ethanol, as shown in Figure 9g.

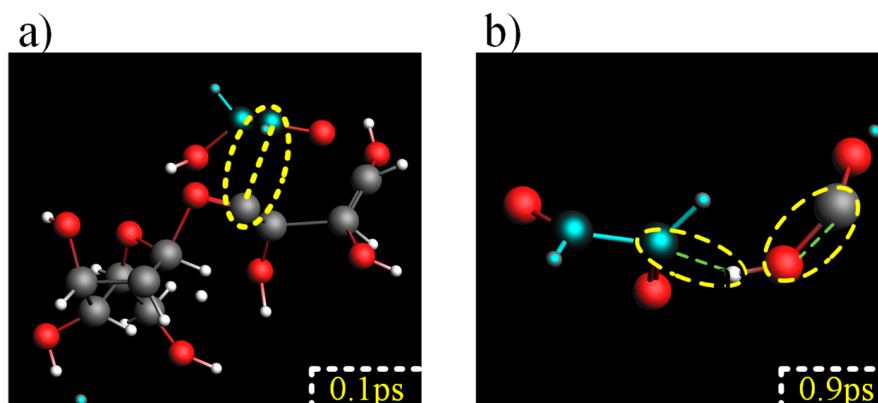


Figure 9. Cont.

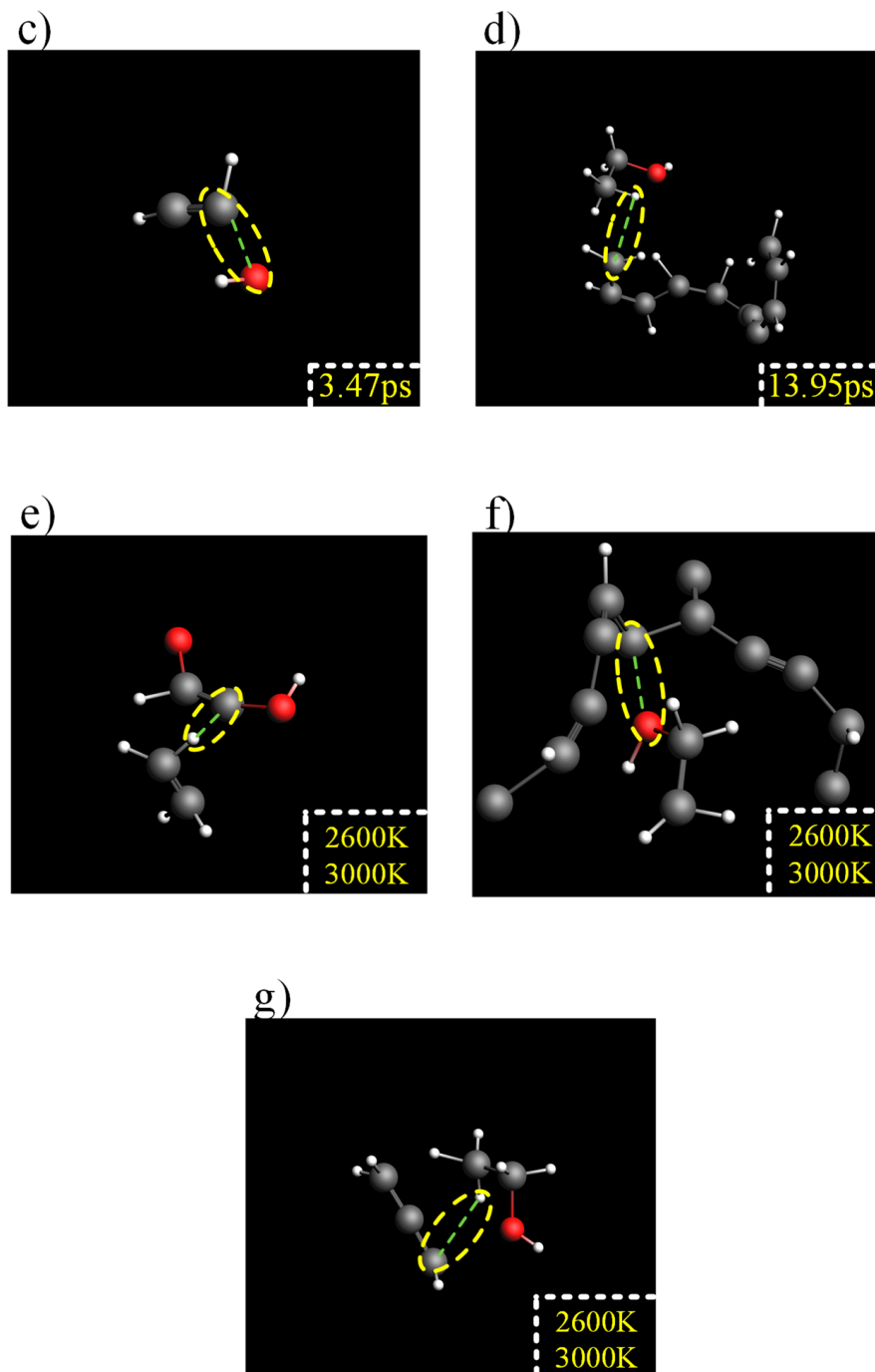


Figure 9. (a–g) The curve of ethanol molecules.

3.3. Analysis on the Solubility of Ethanol

The solubility of ethanol in insulating oil from 298.15 K to 413.15 K was obtained through the calculation of COSMS-RS module. The curve of ethanol solubility is shown in Figure 10. It shows that the solubility of ethanol in insulating oil increased with the increase of temperature. In the case of local hot spots, ethanol did not evaporate due to local high temperature, but was more easily dissolved in insulating oil. This feature reduced the error caused by ethanol volatilization, and enabled power engineers to more accurately correlate the ethanol in oil with the local hot spot aging of transformers. Thus, ethanol can be dissolved in oil stably and not volatilized into transformer voids during the aging process, which would characterize ethanol as an effective aging indicator.

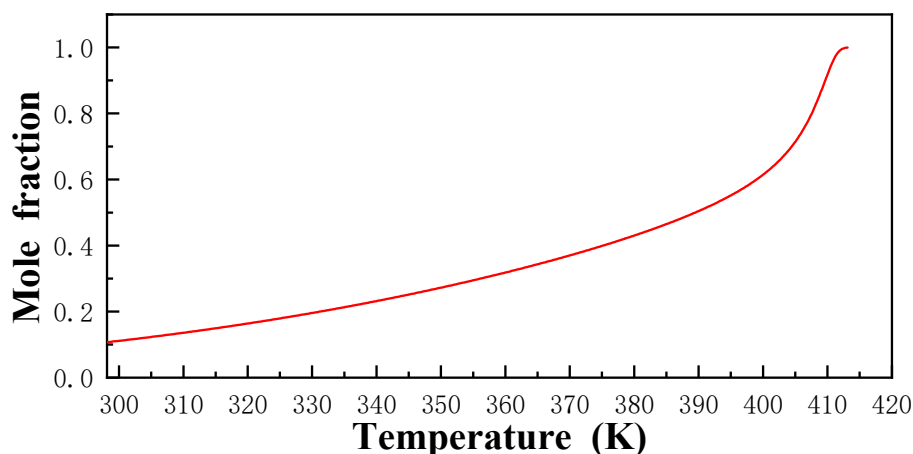


Figure 10. The solubility of ethanol in insulating oil.

4. Conclusions

In this paper, the ReaxFF-MD method was applied to simulate the aging process of oil-immersed transformer insulating paper. The trajectory of ethanol production was studied at the atomic level, and the formation of ethanol at different temperatures was analyzed. The results are shown as follows:

(1) Through the above analysis of molecular trajectory, ethanol mainly came from the intermediate product (vinyl alcohol) of cellobiose pyrolysis. Then vinyl alcohol reacted with other groups to produce ethanol. Therefore, the production of ethanol required a secondary reaction from the intermediate product. However, vinyl alcohol was a very unstable chemical. It would automatically become a mixture of vinyl alcohol and acetaldehyde in reality. Therefore, further research on cellulose intermediates is needed.

(2) According to the production curve of ethanol, no stable ethanol was produced in the early stage of cellobiose pyrolysis. However, the formation of ethanol was stable and existed in the whole middle and late stage. In addition, the solubility of ethanol in oil also indicated that high temperature promoted ethanol to dissolve in insulating oil to reduce the error caused by ethanol volatilization. The increase of temperature is closely related to ethanol. In the actual operation of the transformer, the aging of local hot spots is more serious than that of other areas. Ethanol can better reflect the non-uniform aging condition of transformer insulating paper. Therefore, ethanol has incomparable advantages as an indicator of transformer aging. It can reflect the local hot spots of transformer insulation paper more accurately, especially in the case of local high temperature thermal fault. At the same time, its drawback was that it had poor performance in the early stage and the general thermal aging compared with furfural. Therefore, it is necessary to combine ethanol with other indicators for further investigations to make up for the deficiency of ethanol as an indicator. Meanwhile, this study provides an effective theoretical basis for ethanol as a new aging indicator at the atomic level.

Author Contributions: Y.Z. and S.L. designed the experiments and simulated; Y.L. and H.Z. analyzed the data; Y.L. performed the writing; J.L. contributed the literature search, discussion, and paper modification. All authors have read and agreed to the published version of the manuscript.

Funding: This work was supported by the National Natural Science Foundation of China (51867003; 51907034; 61473272).

Acknowledgments: This work was supported by the National Natural Science Foundation of China (51867003; 51907034; 61473272), the Natural Science Foundation of Guangxi (2018JJB160056; 2018JJB160064; 2018JJA160176), the Basic Ability Promotion Project for Yong Teachers in Universities of Guangxi (2019KY0046; 2019KY0022), the Guangxi Thousand Backbone Teachers Training Program, the Boshike Award Scheme for Young Innovative Talents, and the Guangxi Bagui Young Scholars Special Funding.

Conflicts of Interest: The authors declare no conflict of interest.

References

1. Shang, H.; Xu, J.; Zheng, Z.; Qi, B.; Zhang, L. A Novel Fault Diagnosis Method for Power Transformer Based on Dissolved Gas Analysis Using Hypersphere Multiclass Support Vector Machine and Improved D–S Evidence Theory. *Energies* **2019**, *12*, 4017. [[CrossRef](#)]
2. Zhang, Y.; Fang, J.; Wang, S.; Yao, H. Energy-water nexus in electricity trade network: A case study of interprovincial electricity trade in China. *Appl. Energy* **2020**, *257*, 113685. [[CrossRef](#)]
3. Liu, J.; Fan, X.; Zhang, Y. Temperature Correction on Frequency Dielectric Modulus and Activation Energy Prediction of Immersed Cellulose Insulation. *IEEE Trans. Dielectr. Electr. Insul.* **2019**. [[CrossRef](#)]
4. Zhang, Y.; Li, Y.; Zheng, H.; Zhu, M.; Liu, J.; Yang, T.; Zhang, C.; Li, Y. Microscopic reaction mechanism of the production of methanol during the thermal aging of cellulosic insulating paper. *Cellulose* **2019**. [[CrossRef](#)]
5. Bureau of Indian Standards. *Mineral Oil-Impregnated Electrical Equipment in Services—Guide to the Interpretation of Dissolved and Free Gases Analysis*; Bureau of Indian Standards: New Delhi, India, 2006.
6. Liu, J.; Fan, X.; Zhang, Y. Quantitative evaluation for moisture content of cellulose insulation material in paper/oil system based on frequency dielectric modulus technique. *Cellulose* **2019**, 1–14. [[CrossRef](#)]
7. Gao, Y.; Wang, X.-H.; Yang, H.-P.; Chen, H.-P. Characterization of products from hydrothermal treatments of cellulose. *Energy* **2012**, *42*, 457–465. [[CrossRef](#)]
8. Liu, J.; Fan, X.; Zhang, Y.; Zheng, H. Condition Prediction for Oil-immersed Cellulose Insulation in Field Transformer Using Fitting Fingerprint Database. *IEEE Trans. Dielectr. Electr. Insul.* **2019**. [[CrossRef](#)]
9. Leibfried, T.; Jaya, M.; Majer, N.; Schafer, M.; Stach, M.; Voss, S. Postmortem investigation of power transformers—Profile of degree of polymerization and correlation with furan concentration in the oil. *IEEE Trans. Power Deliv.* **2013**, *28*, 886–893. [[CrossRef](#)]
10. Jalbert, J.; Gilbert, R.; Tétreault, P.; Morin, B.; Lessard-Déziel, D. Identification of a chemical indicator of the rupture of 1, 4- β -glycosidic bonds of cellulose in an oil-impregnated insulating paper system. *Cellulose* **2007**, *14*, 295–309. [[CrossRef](#)]
11. Arroyo-Fernández, O.H.; Fofana, I.; Jalbert, J.; Rodriguez, E.; Rodriguez, L.B.; Ryadi, M. Assessing changes in thermally upgraded papers with different nitrogen contents under accelerated aging. *IEEE Trans. Dielectr. Electr. Insul.* **2017**, *24*, 1829–1839. [[CrossRef](#)]
12. Matharage, S.Y.; Liu, Q.; Davenport, E.; Wilson, G.; Walker, D.; Wang, Z.D. Methanol detection in transformer oils using gas chromatography and ion trap mass spectrometer. In Proceedings of the 2014 IEEE 18th International Conference on Dielectric Liquids (ICDL), Bled, Slovenia, 29 June–3 July 2014; pp. 1–4.
13. Jalbert, J.; Rodriguez-Celis, E.M.; Arroyo-Fernández, O.H.; Duchesne, S.; Morin, B. Methanol Marker for the Detection of Insulating Paper Degradation in Transformer Insulating Oil. *Energies* **2019**, *12*, 3969. [[CrossRef](#)]
14. Rodriguez-Celis, E.M.; Duchesne, S.; Jalbert, J.; Ryadi, M. Understanding ethanol versus methanol formation from insulating paper in power transformers. *Cellulose* **2015**, *22*, 3225–3236. [[CrossRef](#)]
15. Parr, R.G. Density-functional theory. *Chem. Eng. News* **1990**, *68*, 45.
16. Agrawalla, S.; Van Duin, A.C.T. Development and application of a ReaxFF reactive force field for hydrogen combustion. *J. Phys. Chem. A* **2011**, *115*, 960–972. [[CrossRef](#)] [[PubMed](#)]
17. Van Duin, A.C.T.; Dasgupta, S.; Lorant, F.; Goddard, W.A. ReaxFF: A reactive force field for hydrocarbons. *J. Phys. Chem. A* **2001**, *105*, 9396–9409. [[CrossRef](#)]
18. Paaianen, A.; Vaari, J. High-temperature decomposition of the cellulose molecule: A stochastic molecular dynamics study. *Cellulose* **2017**, *24*, 2713–2725. [[CrossRef](#)]
19. Zheng, M.; Wang, Z.; Li, X.; Qiao, X.; Song, W.; Guo, L. Initial reaction mechanisms of cellulose pyrolysis revealed by ReaxFF molecular dynamics. *Fuel* **2016**, *177*, 130–141. [[CrossRef](#)]
20. Zhang, Y.; Wang, X.; Li, Q.; Yang, R.; Li, C. A ReaxFF molecular dynamics study of the pyrolysis mechanism of oleic-type triglycerides. *Energy Fuels* **2015**, *29*, 5056–5068. [[CrossRef](#)]
21. Gao, Z.; Li, N.; Chen, M.; Yi, W. Comparative study on the pyrolysis of cellulose and its model compounds. *Fuel Process. Technol.* **2019**, *193*, 131–140. [[CrossRef](#)]
22. Wang, D.; Zhu, Z.; Zhang, L.; Qian, Y.; Su, W.; Chen, T.; Fan, S.; Zhao, Y. Influence of metal transformer materials on oil-paper insulation after thermal aging. *IEEE Trans. Dielectr. Electr. Insul.* **2019**, *26*, 554–560. [[CrossRef](#)]
23. Mazeau, K.; Heux, L. Molecular dynamics simulations of bulk native crystalline and amorphous structures of cellulose. *J. Phys. Chem. B* **2003**, *107*, 2394–2403. [[CrossRef](#)]

24. Amsterdam Modeling Suite. Scientific Computing & Modelling. Available online: <http://www.scm.com> (accessed on 30 May 2019).
25. Shi, L.; Zhao, T.; Shen, G.; Hou, Y.; Zou, L.; Zhang, L. Molecular dynamics simulation on generation mechanism of water molecules during pyrolysis of insulating paper. In Proceedings of the 2016 IEEE International Conference on High Voltage Engineering and Application (ICHVE), Chengdu, China, 19–22 September 2016; pp. 1–4.
26. MOPAC2016. Stewart Computational Chemistry. Available online: <http://openmopac.net> (accessed on 28 December 2019).
27. Tang, J.; Song, Y.; Zhao, F.; Spinney, S.; da Silva Bernardes, J.; Tam, K.C. Compressible cellulose nanofibril (CNF) based aerogels produced via a bio-inspired strategy for heavy metal ion and dye removal. *Carbohydr. Polym.* **2019**, *208*, 404–412. [[CrossRef](#)] [[PubMed](#)]
28. Zhang, L.; Jiang, L.; Zhao, T.; Zou, L. Microcosmic mechanism investigation on lightning arc damage of wind turbine blades based on molecular reaction dynamics and impact current experiment. *Energies* **2017**, *10*, 2010. [[CrossRef](#)]
29. Chenoweth, K.; Van Duin, A.C.T.; Goddard, W.A. ReaxFF reactive force field for molecular dynamics simulations of hydrocarbon oxidation. *J. Phys. Chem. A* **2008**, *112*, 1040–1053. [[CrossRef](#)] [[PubMed](#)]
30. So/rensen, M.R.; Voter, A.F. Temperature-accelerated dynamics for simulation of infrequent events. *J. Chem. Phys.* **2000**, *112*, 9599–9606. [[CrossRef](#)]
31. Pye, C.C.; Ziegler, T.; Van Lenthe, E.; Louwen, J.N. An implementation of the conductor-like screening model of solvation within the Amsterdam density functional package—Part II. COSMO for real solvents. *Can. J. Chem.* **2009**, *87*, 790–797. [[CrossRef](#)]
32. AMS 2019.3 COSMO-RS, SCM. Theoretical Chemistry. Available online: <http://www.scm.com> (accessed on 30 May 2019).
33. Zhang, Y.; Li, Y.; Zheng, H. Molecular Dynamics Simulation on the Generation of Ethanol for Insulating Paper. In Proceedings of the 6th International Advanced Research Workshop on Transformers (ARWtr), Cordoba, Spain, 7–9 October 2019; pp. 78–82.



© 2020 by the authors. Licensee MDPI, Basel, Switzerland. This article is an open access article distributed under the terms and conditions of the Creative Commons Attribution (CC BY) license (<http://creativecommons.org/licenses/by/4.0/>).